8th International Conference
on
Wind Turbine Noise
Lisbon – 12th to 14th June 2019

Development of Design Guidelines for Low Noise But High Yield Wind Turbines

C. Hornung, Th. Lutz, E. Krämer
Institute of Aerodynamics and Gas Dynamics, University of Stuttgart, Germany

Summary

The reduction of wind turbine noise has been an ongoing effort over the past years, during which a variety of methods were developed. Today the reductions which are the easiest to achieve are already exploited, for example mechanical noise or stall noise is no longer an issue for modern wind turbines. In the audible range basically only trailing edge (TE) noise and inflow noise remain. However, reducing these further is a challenge which, most probably, only myriads of small steps during the whole design process of a turbine will conquer. In the perspective of a silent turbine design, the first steps take place during the design of the airfoils followed by those during the blade design. Subsequently adequate add-ons, for example serrations, and maybe even expensive active noise reduction methods as suction are selected. Finally the operation management must be suitably chosen. The focus of the present study is the aspect of loft design. It aims at the development of universal guidelines for blades with low trailing edge noise emissions but nevertheless high yield. To determine the TE noise, the in-house code IAGNoise+ is employed, which is based on a modified TNO-model. The power is calculated by a blade element method. In order to approach the subject in a structured way, a design of experiment method as developed by Taguchi was chosen. It is conducted for different sections, and thus different airfoils, in the outer part of a reference blade from the TUM reference turbine. The examined parameters are chord, pitch and twist. The analysis focuses on the aeroacoustics and aerodynamics. Restrictions due to loads are assumed to be equal to the reference blade. In can be shown that for each blade section a combination of angles and chord exist, for which an optimum between noise and power is achieved.

1. Introduction

The tonal components in the emitted aeroacoustic sound spectrum of wind turbines are usually amplified by feedback loops or periodic vortex separation. They are thus based on distinct processes, which can be manipulated relatively easy in order to reduce the noise emission. The broadband part of the spectrum, however, which is related to interactions of the blade with turbulence is significant more challenging to reduce. Positively influencing the complex mechanisms underlying the turbulence production and dissipation in order to reduce the noise sources is extremely challenging. Thus, the prevailing sound source in the audible range of the emitted spectra from wind turbines is still the turbulence induced trailing edge noise (short: TE noise). Over the years various methods have been proposed in literature to conquer TE noise.

Already during the design of the airfoils, attention should be paid to a noise-optimised design by keeping the turbulent length scale and the turbulent kinetic energy close to the TE as low as possible, in particular on the suction side. This is achieved by delaying the laminar to turbulent transition, but at the same time avoid separation bubbles. In addition it should be aimed for a soft pressure recovery by balancing the pressure regain between suction and pressure side [15]. Rautmann [18] suggest the use of a concave suction side close to the TE and a shift of load to the pressure side by using rear loading to compensate for the loss in lift. [18]. Different authors achieve noise reduced airfoils by utilizing optimization routines paired with semi-empirical or computational aeroacoustics (CAA) methods. Compared to the baseline airfoils, noise reductions by more than 2 dB are obtained. [2, 13, 21]

The blades of the rotor are then designed based on the set of (noise-optimised) airfoils. In all studies found, in which the noise reduction of the rotor is compared to the reduction of the airfoil itself, a lower or no noise reduction was measured for the rotor compared to the optimized airfoil only. This makes it clear that it is of great relevance how exactly the rotor is assembled from the blade sections. Some studies have already dealt with the topic and improved the geometry of individual rotors with the help of an optimization routine. Most of the optimized rotors had slightly larger chord and an increased twist angle than the baseline versions. [3, 5, 13, 14, 21].

A commonly chosen method to reduce noise emission in particular for already built turbines is to modify the operation mode. Since TE noise scales with the fifth power of the inflow Ma number, a reduction of rpm and thus the tip speed ratio immediately reduces the noise emission. However, as pointed out by [3] this results in higher loads on generator or gearbox and is thus only feasible within a small range without changing to a more expensive drive train.

Further noise reductions are achieved with so called add-ons. Serrations are already state-of the art. Almost all manufacturers now equip the blades with them as standard. The narrow triangles attached to the TE showed very promising results in wind tunnel test, where reductions of up to 6 dB were achieved. On the rotor, however, the reduction is less pronounced with 2 -3 dB [17]. Novel approaches include different forms of serrations, leaving the classical triangle behind, porous TE, combed serrations or even only combs. In particular the latter ones have proven significant effect in wind tunnel measurements. [4, 8, 17, 19, 20]

In addition, active methods are also investigated in research. Since they are usually associated with considerable costs for additional systems and it is difficult to design additional systems for the long operating life of wind turbines over several decades, so far, they have only been used in experimental studies. For example, the boundary layer on the suction side of the blade can be sucked in through a perforated plate to reduce the boundary layer thickness and the turbulent kinetic energy at the TE [1].

An alternative method is to influence the boundary layer by plasma actuators. [12]
To reach the goal of silent but at the same time power and cost efficient turbines, different described methods have to be combined. The least complex approaches are now used as standard and have already led to a significant reduction in noise emission. In order to further reduce trailing edge noise, it is inevitable to consider the noise mechanisms in the entire design process of the turbine.

The work presented here addresses the blade design process. Instead of optimizing a specific rotor, as is the case in the literature (see above), the goal is the development of general guidelines for blade design for low noise but nonetheless high yield. For this purpose two different turbines were examined, one of them is a commercial multi-megawatt turbine, the other is the TUM reference turbine designed in the framework of the IEA wind task 37 [3]. The results of the study are illustrated at the example of the reference turbine, but the conclusions drawn coincided for both turbines which supports the universality of the guidelines. To make the study more efficient a structured approach is chosen based the Taguchi method, a Design of Experiment (DoE) approach [7]. In addition, rather than examining the whole blade with multiple influencing parameters, it was focused on certain blade sections, similar to the blade element method (BEM) commonly used for power based turbine design.

The paper is structured as follows: Section 2 explains the general procedure followed, as well as the theory behind the noise and power prediction method employed. Afterwards the results of the approach are presented and the derivation of general guidelines is discussed in section 3. The conclusions drawn from the study for blade design are summarized at the end of the paper.

2. Methods

The TUM reference turbine is a model turbine with a rotor diameter of 130 m and a rated power of 3.6 MW at a tip speed ratio (TSR) of 8.869 [3]. With a cut in wind speed of 3 m/s the turbine is explicitly designed for use in low wind conditions, where noise emission plays an increased role due to low background noise. The blades are constructed on the basis of a DU airfoil series.
Instead of examining the whole blade, as conducted by the studies presented above, only sections of a blade are considered in the present work. The benefit of this quasi-2D approach is a faster evaluation and a significant reduction of the number of factors influencing the noise emission. Since the TE noise stemming from the outer part of the rotor prevails the overall spectrum the study is concentrated on two blade cuts with different relative thicknesses at 75 % and 98 % of the rotor diameter, which corresponds to a DU91-W2-250 and a DU08-W-210 airfoil, respectively. The highest elevation of emitted noise over background noise is found near the operating point for rated power. Below that point, rpm and thus tip speeds are smaller, leading to lower noise emission because of the Ma^5 scaling of TE noise and above the background noise increases, because of higher wind speeds. Thus, this point was selected for the here presented analysis. The reader has to keep in mind that the study is performed with the goal of a power and sound optimized turbine for low to rated power operating conditions. Restrictions due to structure or load as well as due to negative stall effects at very high wind speeds or fluttering at stand still are not taken into account. These effects of course determine the boundary conditions of the aerodynamically-acoustically optimized turbine in an industrial development process.

2.1. Procedure

A section at any position along the blade can be described with the parameters depicted in figure 1 and the airfoil's geometry. Keeping the airfoil as well as the position along the blade constant and implying constant TSR and wind speed, two independent parameters, chord c and angle of incidence ξ, remain. Note that the angle towards the undisturbed flow is not equal to the angle of attack experienced by the airfoil. The parametric study is thus conducted by varying angle of incidence and chord for the two different sections. In order to evaluate the influence of both parameters as well as

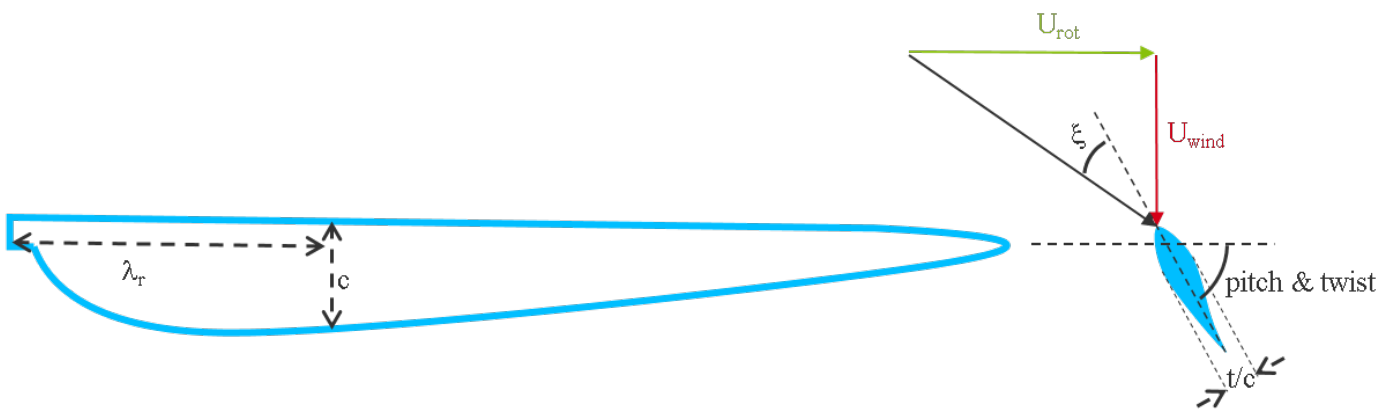

Fig. 1 Visualization of the quasi 2D approach with blade segments.

the interaction, the Taguchi method is employed. Different pre-desigend test matrices are available for this purpose, which satisfy the conditions of orthogonality and balance of the test design. Here the $L_{25}(5^6)$ matrix was used (cf. [7]). It comprises 25 different simulations, each with different settings. The two parameters, chord and angle of incidence were varied with 5 steps (levels) for each. Only the first two columns of the Taguchi test matrix were occupied, which makes it possible to evaluate the interactions between chord and angle of incidence. An overview over the range of the selected levels is given in table 1. The upper and lower boundaries for the chord were set to reasonable numbers around the design chord length but trying to explore the available space. The range for the angle of incidence were selected in such a way, that the lowest occurring lift coefficient was only just positive and the highest was close to stall (for the design Re number). The levels in between were equally spaced. After the evaluation of this first quite rough matrix, it was decided to define three further more refined matrices by selecting the most promising parameter ranges according to the matrix with the rough steps. For each combination of chord and angle of incidence the local power coefficient $C_{p,2D}$ and the local sound pressure level (SPL) are determined with respect to a spanwise width of the segment of 1 m. The power coefficient is calculated by means of the blade element method (BEM) (cf. section 2.4) and the SPL is predicted utilizing the in-house code IAGNoise+ based on RANS CFD simulations (cf. section 2.3). The inflow conditions for the RANS simulations are also gained from the BEM to consider the effects of induction on the noise emission. The results of the rough test matrices are then examined based on the Taguchi method. Afterwards the three refined matrices were defined for each section, in order to extract general design guideline.

DU08-W-210 (rad pos.: 98 %)				
	coarse	fine 1	fine 2	fine 3
Chord [m]	0.1 - 1.7	1.3 - 1.7	0.1 - 0.9	0.1 - 0.9
Angle of incidence [°]	(-6.0) - 9.0	1.5 - 5.25	(-6.0) - 1.5	1.5 - 5.25

DU91-W2-250 (rad pos.: 75 %)				
	coarse	fine 1	fine 2	fine 3
Chord [m]	0.5 - 2.6	1.75 - 2.375	0.5 - 1.75	0.5 - 1.75
Angle of incidence [°]	(-3.0) - 11.0	4.0 - 7.5	(-3.0) - 4.0	4.0 - 7.5

Table 1 Test matrices for the parametric study.

2.2. CFD simulations

CFD simulations were conducted to gain the polars for the BEM as well as for each test case to determine the noise. The simulations were conducted with the structured, compressible solver FLOWer, developed by the DLR and extended by the IAG. In order to use the same grid for all simulations of one airfoil a very fine mesh was designed consisting of approximately 0.15 Mio. cells in 18 Blocks. It was ensured that for all simulations the y^+ value in the cell closest to the wall is smaller than 1 and the cells expand with a ratio of 1.1 in wall normal direction. The far field was set to a distance greater than 80 chord lengths. To depict the effects of turbulence the two equation Menter SST Turbulence model was employed for the fully turbulent simulations.

2.3. Noise prediction

The noise is predicted using the in-house code IAGNoise+ [9]. Roughly sketched, the procedure can be divided in three steps: First boundary layer data close to the TE is extracted from a RANS CFD simulation. The data is then processed with statistical methods to determine the wall pressure fluctuations, employing a TNO type model. These type of models are based on a semi-analytical expression describing the power density of the frequency wave number spectrum of the wall pressure fluctuations (WPF) in dependence from turbulence characteristics. It is derived from a Poisson equation for pressure fluctuations via the use of a Greens-Function and Powel's reflection theorem. The turbulence characteristics are described with spectral model parameters. Within IAGNoise+ an enhanced version of the TNO model is implemented [9]. The governing equation for the power spectral density of the wall pressure fluctuations is:

$$P\left(k_1, k_3, \omega\right) = 4\rho^2 \left(\frac{1}{k_1^2 + k_3^2}\right) \cdot \int_0^\infty \left(k_1^2 \left(\frac{\partial \overline{U_1}}{\partial x_2}\right)^2 + \frac{2\left(k_1^2 + k_3^2\right)}{15\nu}\varepsilon\right) \Lambda_2 \Phi_{22} \cdot \langle {u_2'}^2 \rangle \Phi_m e^{-2|\mathbf{k}|x_2} dx_2 \tag{1}$$

In the equation ρ represents the density, the wave-numbers in stream-wise, wall normal and span-wise direction are depicted by k_1, k_2, k_3 , respectively. The frequency is represented by ω. The vertical integral length scale Λ_2 is a measure for the size of the energy containing eddies in the boundary layer

and the moving axis spectrum Φ_m describes the distortion of the spectrum when being convected in direction of the TE. The normalized spectrum of the vertical velocity fluctuations is given by Φ_{22} with the corresponding Reynolds stresses $\langle u_2'^2 \rangle$. Further model parameters are the dissipation ε and the viscosity ν. Compared to the original model it takes not only the interactions between the turbulence and the mean shear into account but also the interaction amongst the turbulence itself. Further, the anisotropy of the turbulent fluctuations is accounted for based on the approach by Kamruzzaman [11], but considering pressure gradients. Several smaller modifications include a different approach for the moving axis spectrum or the length scales. As a last step the results of the WPF model are fed into a far field model to determine the sound pressure level. All equations can be found in [9]. All in all, the different modifications improved the prediction quality of the model, in particular for high lift configurations. It has been shown, that with the current model it is possible to predict the noise of wind turbine rotors to a good degree of certainty. The CFD simulations were evaluated very close to the TE at 99,5 % of the chord. Predicting the noise in combination with FLOWer CFD SST simulations have been shown to gain good results for turbines as well as for airfoils [9, 10].

2.4. BEM

The airfoil polars, which are required for the BEM, are determined with the CFD code FLOWer. They were calculated for the design Reynolds number of 6 Mio. for the DU08-W-210 and 8 Mio. for the DU91-W2-250. Since the inflow conditions change in the course of the parameter study, the Reynolds number changes as well. However, the deviations due to differing Reynolds numbers for the different settings in the parametric study is neglected. The just-in-time calculation of polars with XFOIL with the exact required Reynolds number showed a larger difference to the final lift coefficient of the subsequent FLOWer simulation. Upon convergence of the CFD simulations the TE noise emission of each section is predicted with IAGNoise+. The contribution of each section to the overall power of the turbine is evaluated by a BEM formulation for the local power coefficient. For a whole turbine the power coefficient can be determined via (cf. e.g. [16]):

$$C_P = \frac{8}{\lambda^2} \int_{\lambda_h}^{\lambda} \lambda_r^3 a'(1-a) \left[1 - \frac{c_d}{c_l} tan\phi \right] d\lambda_r \tag{2}$$

The local power coefficient of each section with respect to 1 m $C_{P,2D}$ is calculated by breaking down the continuous integral for the overall rotor C_p in eq. (2) to discrete sections, resulting in:

$$\begin{aligned} &C_{P,2D} = \frac{8}{\lambda^2} \lambda_r^4 a'(1-a) \left[1 - \frac{c_d}{c_l} tan\phi \right] \Delta\lambda_r \\ &with \\ &\Delta\lambda_r = (\lambda_r(r+0.5m) - \lambda_r(r-0.5m)) \end{aligned} \tag{3}$$

In the equations a describes the axial induction whereas a' represents the tangential induction. The tip speed ratios at the hub, any radial position and the tip are denoted by λ_H, λ_r, λ, respectively. The lift- and drag coefficients are represented by c_l and c_d. In addition, the angle to the local inflow (including induction effects) φ is required to calculate the power coefficients.

3. Results and Discussion

In figure 2 the results of all test matrices are plotted. Shown are the local power coefficients over the axial induction colored by the total sound pressure level. Data points with an induction factor greater than 0.4 are excluded, since the classical BEM method is prone to errors for these induction factors (cf. also [6]). The symbols with lower $C_{P,2D}$ correspond to the DU91-W2-250 airfoil whereas the higher located points stem from the simulations with the DU08-W-210 airfoil. Besides few exceptions, the noise emission can be observed to increase with rising induction factor. The local power coefficient, however, shows a maximum at approximately 0.33, as expected from Betz's theory, and then decreases again. Therefore, over-induced turbines are associated with a higher noise emission for the same power coefficient. Thus, while an over-induction may be useful to maximize the energy yield for gusty inflow, this approach is not advisable for low-noise turbines.

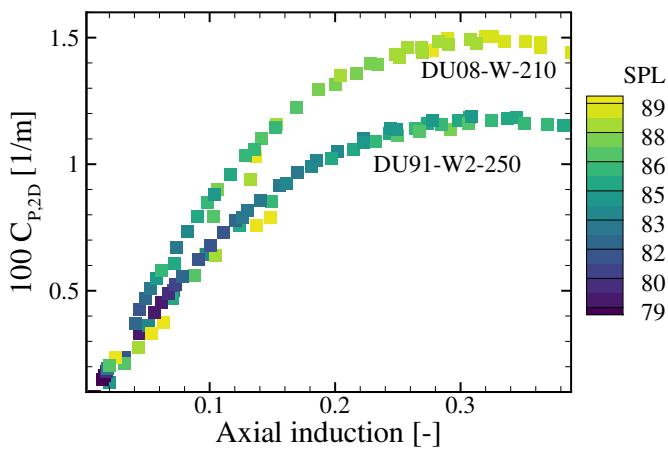

Fig. 2 Local power coefficient and SPL for both airfoils.

The strength of the Taguchi method lays in its statistical evaluation. Here the Analysis of Mean (ANOM) procedure is pursued. It was adapted by Taguchi to the orthogonal fields. It allows for an estimation of the tendency of the different parameters over the range of levels. In addition the influence of different factors can be compared. Thus, it gives an idea of the direction for optimization.[7] The analysis is shown in figure 3 for the coarse test cases only (cf. table 1). They comprise the widest range of both parameters and are thus more suitable to evaluate trends. Note that all points were included in the analysis, also those with induction factors larger than 0.4. However, since the trends are depicted by the BEM also for high induction factors, the overall tendencies shown in the plots should still be valid. On the left (fig. 3(a)) the results are depicted for the SPL. The grey dashed line shows the overall mean value. The green line focuses on the variation of the chord. Each point on the line represents the mean value over those simulations in which the chord length is set to the corresponding level. The conclusion can be drawn from the plot, that with higher chord length the SPL increases in average. This holds for both airfoils. The blue line shows the level averaged behaviour for the influence of the incidence angle. In contrast to the chord, here a local minimum can be observed. Overall the influence of the incidence angle is greater than that of the chord. The reason for the maximum being located at level five for the DU08-W-210 airfoil but at level one for the DU91-W2-250 airfoil lays in the greater contribution of the pressure side's noise emission at low angle of attack for the latter airfoil.

Turning the attention to the right handed figure (fig. 3(b)), shows the same analysis but now for the local power coefficient. The range of the parameters can be considered sufficient to find optimal points, since also here the maximum can be observed although the levels were chosen somewhat arbitrarily. For the DU08-W-210 airfoil it coincides for the factor of chord and angle at level four. For the thicker airfoil, DU91-W2-250, the maximum of the chord is located at level two, and the maximum for the angle at level four. As expected, the optimum levels in angle differ for SPL and $C_{P,2D}$, indicating

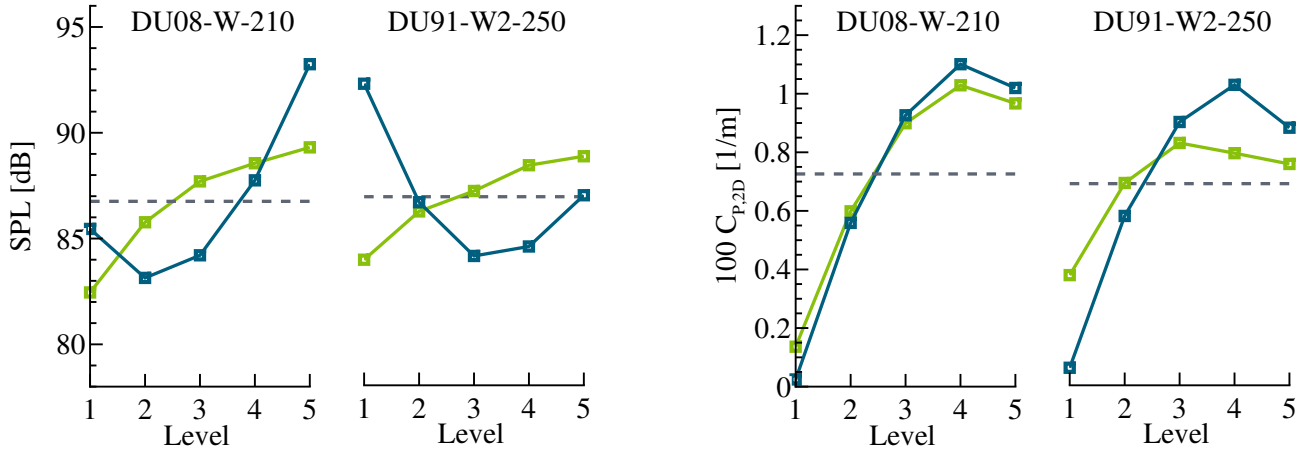

(a) ANOM SPL Caption (b) ANOM Cp Caption

Fig. 3 ANOM for SPL and $C_{P,2D}$ with the overall mean value --, the influence of the chord -□- and of the angle of incidence -□-.

a Pareto front problem.
The ANOM separates the influence of different factors. The interaction between the two parameters can then be graphically evaluated as shown in figure 4.

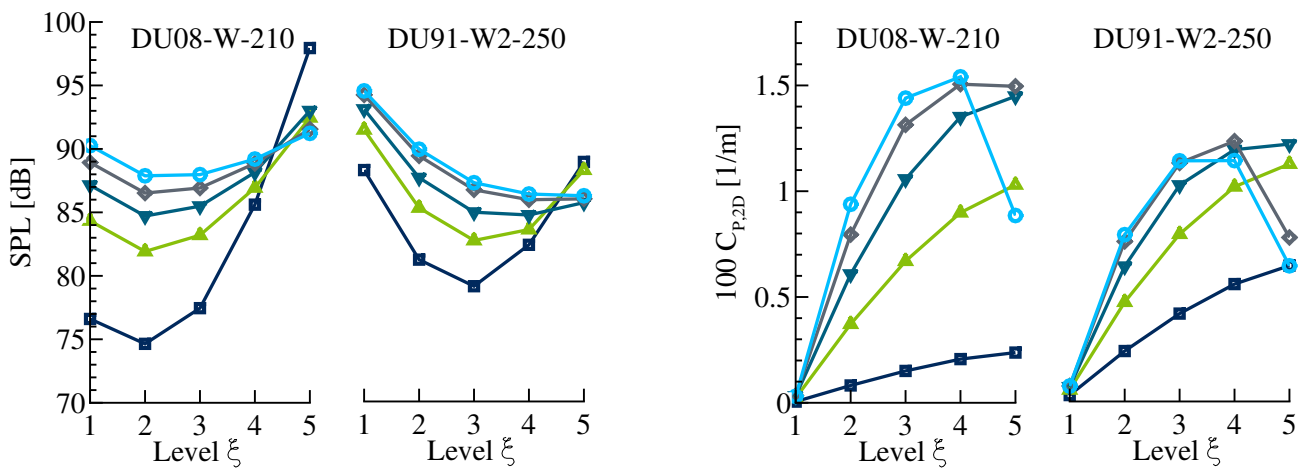

(a) SPL (b) Cp

Fig. 4 Interaction diagram according to Taguchi with chord level 1 -□-, level 2 -△-, level 3 -▽-, level 4 -◇-, level 5 - ○ -.

Depicted are the results with the different levels of the angle of incidence on the abscissa. The different lines represent the levels of the chord length with dark blue being the smallest chord and bright blue representing the largest. Parallel curves would indicate that no interactions are present. Here, the directing of the curves stays the same over the lower range of levels for C_P as well as for

SPL. Thus, the parameters have synergetic interactions. An increase in chord leads to a similar result as an increase in angle of incidence. It can be concluded that both parameters have to be modified to achieve a low noise - high yield configuration.
In order to determine the best operating points for each airfoil, the results of all test matrices, including the refined ones are evaluated (cf. table 1). Points with induction factors higher than 0.4 are again excluded for the above mentioned reasons and because of their lack of relevance for real turbine design. In figure 5 the difference in local power coefficient and SPL between the original design and the simulations of the test matrices are depicted. They are defined as:

$$\Delta SPL = SPL_{test} - SPL_{design} \qquad \Delta C_{P,2D} = C_{P,2D,test} - C_{P,2D,design} \tag{4}$$

All points are colored by their corresponding lift-to-drag ratio, with the lift and drag coefficients taken from the polars of the design configuration. While the DU91-W2-250 airfoil is already operated in an

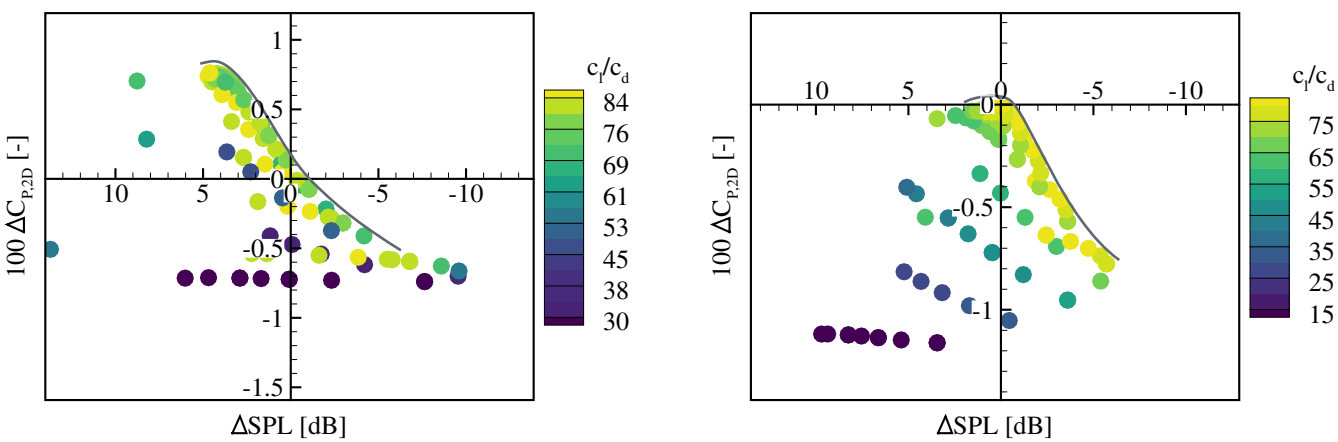

(a) DU08-W-210

(b) DU91-W2-250

Fig. 5 Pareto front for low noise -high yield design of the two sections, depicted as deviation from the original TUM design.

optimal design point in the reference turbine, there is still a little bit of potential in noise reduction for the DU08-W-210 airfoil. For both airfoils a point of maximum possible power can be determined. As typical for optimization problems a Pareto front forms out (grey line). Points located close to the line are characterized by the lowest possible noise emission for a certain local power coefficient for one distinct airfoil. It stands out that the airfoils are operated in their highest lift-to-drag ratio point when being close to the optimal line. The results for the DU08-W-210 airfoils are, however, influenced by Re number effects. Some data points with high lift-to-drag ratio are located slightly away from the Pareto front. They are, however, associated with the smallest tested chord length, which's Re number is only 20% of the design Re used to determine the polars.

4. Conclusion

A parametric study was conducted based on the blade and airfoil design from the TUM reference turbine to develop general guidelines for blades with low trailing edge noise emissions but nevertheless high yield. To facilitate the evaluation as well as computational time a quasi-2D approach was used. Two different sections, corresponding to two different radial positions and airfoil geometries were examined. Two different parameters were varied: The incidence angle (inclination towards the undisturbed inflow from pitch and twist) and the chord length. From the results several conclusions were drawn for the development of silent but powerful wind turbines. The most important being that for low noise wind turbines small effective angles of attack should be combined with high chord lengths aiming to operate the airfoils at their highest lift-to-drag-ratio point. Thus, for each radial position-airfoil combination a setting exists leading to the point of maximum power with minimal noise. These points are characterized by small effective angles of attack and high chord lengths. Over-induction should in general be avoided since it leads to higher noise only without increasing the power output. Restrictions due to structure or load as well as due to negative stall effects at very high wind speeds or fluttering at stand still were not taken into account.

Acknowledgments

Parts of this work were supported by Enercon GmbH Aurich. Further, we thank Pietro Bortolotti (previously University of Munich, now at NREL) for providing us with the geometry of the TUM reference turbine.

References

[1] Arnold, B., Lutz, T., and Krämer, E. (2018). Design of a Boundary-Layer Suction System for Turbulent Trailing-Edge Noise Reduction of Wind Turbines. *Renewable Energy Journal*, 123:249–262.

[2] Bertagnolio, F., Madsen, H. A., and Bak, C. (2009). Experimental Validation of TNO Trailing Edge Noise Model Validation and Application to Airfoil Optimization. In *EWEC Proceedings online*.

[3] Bortolotti, P., Sucameli, C., Croce, A., and Botasso, C. (2018). Integrated design optimization of wind turbines with noise emission constraints Integrated design optimization of wind turbines with noise emission constraints. In *IOP Conf. Series: Journal of Physics: Conf. Series 1037 (TORQUE)*.

[4] Braun, K. A., Gordner, A., v.d. Borg, N., Dassen, A., Doorenspleet, F., and Parchen, R. (1998). Final Report: Serrated Trailing Edge Noise (STENO). Technical report.

[5] Fuglsang, P. and Madsen, H. A. (1998). Wind turbine design with numerical optimization and a semi-empirical noise prediction model.

[6] Guma, G., Bangga, G., Jost, E., Lutz, T., and Kräemer, E. (2018). Consistent 3D CFD and BEM simulations of a research turbine considering rotational augmentation. In *Torque Proceedings*.

[7] Henes, J. D. (2009). *Anwendung der Taguchi-Methode zur Quantifizierung von Fehler- und Unsicherheitsquellen der numerischen Aerodynamik*. Studienarbeit, Stuttgart.

[8] Herr, M., Rossignol, K.-S., Delfs, J., Lippitz, N., and Mößner, M. (2014). Specification of Porous Materials for Low-Noise Trailing-Edge Applications. *20th AIAA/CEAS Aeroacoustics Conference*, (June):1–19.

[9] Hornung, C., Lutz, T., and Krämer, E. (2019). A model to include turbulence-turbulence interaction in the prediction of trailing edge far fi eld noise for high angles of attack or slightly separated fl ow. 136:945–954.

[10] Hornung, C., Scheit, C., Napierala, C., Arnold, M., Bekiropoulos, D., Altmikus, A., and Lutz, T. (2017). Predicted and Measured Trailing-Edge Noise Emission for a 2.3 MW Wind Turbine. In *7th International Conference on Wind Turbine Noise*, Rotterdam.

[11] Kamruzzaman, M., Bekiropoulos, D., Wolf, A., Lutz, T., and Kramer, E. (2014). Rnoise: A RANS based airfoil trailing-edge noise prediction model. *AIAA conference*, pages 1–22.

[12] Koike, S., Kato, H., Kobayashi, H., Ura, H., Mitsuo, K., Atobe, T., Okubo, T., Nakakita, K., Watanabe, S., Tunnel, W., Researcher, A. S., Group, F. D., Researcher, S., Student, G., Tokyo, S.-k., and Leader, G. (2010). Time-Resolved PIV Applied to Trailing-Edge-Noise Reduction by DBD Plasma Actuator. *27th AIAA Aerodynamic Measurement Technology and Ground Testing Conference*, (July):AIAA 2010–4352.

[13] Lee, S., Lee, S., Ryi, J., and Choi, J.-s. (2013). Design optimization of wind turbine blades for reduction of airfoil self-noise. *Journal of Mechanical Science and Technology*, 27(2):413–420.

[14] Leloudas, G., Zhu, W. J., Sørensen, J. N., Shen, W. Z., and Hjort, S. (2007). Prediction and Reduction of Noise from a 2.3 MW Wind Turbine. *Journal of Physics: Conference Series*, 75(October 2005):012083.

[15] Lutz, T., Herrig, A., Würz, W., Kamruzzaman, M., and Krämer, E. (2007). Design and Wind-Tunnel Verification of Low-Noise Airfoils for Wind Turbines. *AIAA Journal*, 45(4):779–785.

[16] Moriarty, P. J. and Hansen, A. (2005). AeroDyn Theory Manual. Technical Report January, NREL - National Renewable Energy Laboratory.

[17] Oerlemans, S., Fisher, M., Maeder, T., and Kögler, K. (2009). Reduction of Wind Turbine Noise Using Optimized Airfoils and Trailing-Edge Serrations. *AIAA Journal*, 47(6):1470–1481.

[18] Rautmann, C. (2017). Numerical Simulation Concepts for Low-Noise Wind Turbine Rotors, Forschungsbericht 2017-35. Technical report, Deutsches Zentrum f"ur Luft und Raumfahrttechnik.

[19] Rubio Carpio, A., Avallone, F., and Ragni, D. (2018). On the Role of the Flow Permeability of Metal Foams on Trailing Edge Noise Reduction. *2018 AIAA/CEAS Aeroacoustics Conference*.

[20] van der Velden, W. C. and Oerlemans, S. (2017). Numerical study on combed teeth serrations for wind turbine noise reduction. *23rd AIAA/CEAS Aeroacoustics Conference*.

[21] Zhu, W. J., Shen, W. Z., and Sorensen, J. N. (2016). Low - Noise Airfoil and Wind Turbine Design. In *Wind Turbines - Design, Control and Applications*, pages 55–72.